Supplement to "Tests for the existence of group effects and interactions for two-way models with dependent errors"

Yuichi Goto[*,†] Kotone Suzuki[‡,§] Xiaofei Xu[¶,‖] Masanobu Taniguchi[**,††]

This is a supplementary material of the article "Tests for the existence of group effects and interactions for two-way models with dependent errors". In this supplementary material, we provide proofs of our theorems and additional simulation results.

A Proof Section

This section provides all proofs of Theorems in the main manuscript.

The following lemma is the essential tool to show our theorems (Rao and Mitra, 1971, Theorem 9.2.3, p.173).

Lemma A.1. *If $\mathcal{Z}$ follows $N(\mathfrak{m}, \mathcal{V})$, then it holds that $\mathcal{Z}^\top \mathcal{V}^- \mathcal{Z}$ follows the noncentral chi-square distribution with rank$(\mathcal{V})$ degrees of freedom and noncentrality parameter $\mathfrak{m}^\top \mathcal{V}^- \mathfrak{m}$, where $\mathcal{V}^-$ denotes the Moore–Penrose inverse of $\mathcal{V}$.*

A.1 Proof of Theorem 21

First, we shall show, under H_α that $\sqrt{n}\left(\overline{\boldsymbol{y}_{1..}}^\top - \overline{\boldsymbol{y}_{...}}^\top \quad \ldots \quad \overline{\boldsymbol{y}_{a..}}^\top - \overline{\boldsymbol{y}_{...}}^\top\right)^\top$ converges in distribution to ap-dimensional centered normal distribution with the variance $\boldsymbol{V}_\alpha$. For any $i \in \{1, \ldots, a\}$, it holds that $\sqrt{n}\mathbb{E}(\overline{\boldsymbol{y}_{i..}} - \overline{\boldsymbol{y}_{...}}) = \boldsymbol{0}$. We observe that, for any $i_1, i_2 \in \{1, \ldots, a\}$,

$$n\mathrm{Cov}(\overline{\boldsymbol{y}_{i_1..}} - \overline{\boldsymbol{y}_{...}}, \overline{\boldsymbol{y}_{i_2..}} - \overline{\boldsymbol{y}_{...}}) = n\mathrm{Cov}(\overline{\boldsymbol{e}_{i_1..}} - \overline{\boldsymbol{e}_{...}}, \overline{\boldsymbol{e}_{i_2..}} - \overline{\boldsymbol{e}_{...}}) = {}^{n,\alpha}\boldsymbol{V}_{i_1 i_2},$$

where

$$\begin{aligned} {}^{n,\alpha}\boldsymbol{V}_{i_1 i_2} := & \frac{1}{nb^2} \sum_{j_1, j_2 = 1}^{b} \frac{1}{\rho_{i_1 j_1}\rho_{i_2 j_2}} \sum_{t_1=1}^{n_{i_1 j_1}} \sum_{t_2=1}^{n_{i_2 j_2}} \boldsymbol{\Gamma}^{i_1 i_2}_{j_1 j_2}(t_1 - t_2) \\ & - \frac{1}{nab^2} \sum_{s=1}^{a} \sum_{j_1, j_2=1}^{b} \left(\sum_{t_1=1}^{n_{s j_1}} \sum_{t_2=1}^{n_{i_2 j_2}} \frac{1}{\rho_{s j_1}\rho_{i_2 j_2}} \boldsymbol{\Gamma}^{s i_2}_{j_1 j_2}(t_1 - t_2) + \sum_{t_1=1}^{n_{i_1 j_1}} \sum_{t_2=1}^{n_{s j_2}} \frac{1}{\rho_{i_1 j_1}\rho_{s j_2}} \boldsymbol{\Gamma}^{i_1 s}_{j_1 j_2}(t_1 - t_2) \right) \end{aligned}$$

[*]Department of Mathematical Sciences, Faculty of Mathematics, Kyushu University, 744 Motooka, Nishi-ku, Fukuoka, 819-0395, Japan
[†]yuichi.goto@math.kyushu-u.ac.jp
[‡]Department of Pure and Applied Mathematics, Graduate School of Fundamental Science and Engineering, Waseda University, 3-4-1 Okubo, Shinjuku-ku, Tokyo, 169-8555, Japan
[§]va.1016koto@akane.waseda.jp
[¶]Department of Probability and Statistics,Wuhan University, 299 Ba Yi Road, Wuchang District, Wuhan, Hubei, 430072, P.R. China
[‖]xiaofeix@whu.edu.cn
[**]Faculty of Science and Engineering, Waseda University, 3-4-1 Okubo, Shinjuku-ku, Tokyo, 169-855, Japan
[††]taniguchi@waseda.jp

$$+\frac{1}{na^2b^2}\sum_{s_1,s_2=1}^{a}\sum_{j_1,j_2=1}^{b}\frac{1}{\rho_{s_1j_1}\rho_{s_2j_2}}\sum_{t_1=1}^{n_{s_1j_1}}\sum_{t_2=1}^{n_{s_2j_2}}\boldsymbol{\Gamma}_{j_1j_2}^{s_1s_2}(t_1-t_2)$$

with $\boldsymbol{\Gamma}_{j_1j_2}^{i_1,i_2}(h) := \mathbb{E}(\boldsymbol{e}_{i_1j_1t+h}\boldsymbol{e}_{i_2j_2t}^\top)$. From (A1), we can see that ${}^{n,\alpha}\boldsymbol{V}_{i_1i_2}$ converges to ${}^{\alpha}\boldsymbol{V}_{i_1i_2}$ as $\min_{\substack{i=1,\ldots,a\\j=1,\ldots,b}} n_{ij} \to \infty$. For any $\ell \geq 3$, $(i_1,\ldots,i_\ell) \in \{1,\ldots,a\}^\ell$, $(j_1,\ldots,j_\ell) \in \{1,\ldots,b\}^\ell$, and $(d_1,\ldots,d_\ell) \in \{1,\ldots,p\}^\ell$, we found, by (A1), that

$$\begin{aligned}
& n^{\ell/2}\mathrm{Cum}\{\overline{e_{i_1j_1.d_1}},\ldots,\overline{e_{i_\ell j_\ell.d_\ell}}\}\\
&= \frac{n^{-\ell/2}}{\rho_{i_1j_1}\cdots\rho_{i_\ell j_\ell}}\sum_{t_1=1}^{n_{i_1j_1}}\cdots\sum_{t_\ell=1}^{n_{i_\ell j_\ell}}|\mathrm{Cum}\{e_{i_1j_1t_1d_1},\ldots,e_{i_\ell j_\ell t_\ell d_\ell}\}|\\
&= \frac{n^{-\ell/2}}{\rho_{i_1j_1}\cdots\rho_{i_\ell j_\ell}}\sum_{t_1=1}^{n_{i_1j_1}}\sum_{s_2=1-t_1}^{n_{i_2j_2}-t_1}\cdots\sum_{s_\ell=1-t_1}^{n_{i_\ell j_\ell}-t_1}|\kappa_{i_1\cdots i_\ell}^{j_1\cdots j_\ell}(s_2,\ldots,s_\ell;d_1,\ldots,d_\ell)|\\
&\leq \frac{n^{-\ell/2}}{\rho_{i_1j_1}\cdots\rho_{i_\ell j_\ell}}\sum_{t_1=1}^{n_{i_1j_1}}\sum_{s_2=-\infty}^{\infty}\cdots\sum_{s_\ell=-\infty}^{\infty}|\kappa_{i_1\cdots i_\ell}^{j_1\cdots j_\ell}(s_2,\ldots,s_\ell;d_1,\ldots,d_\ell)|\\
&= \frac{n^{-\ell/2+1}}{\rho_{i_2j_2}\cdots\rho_{i_\ell j_\ell}}\sum_{s_2=-\infty}^{\infty}\cdots\sum_{s_\ell=-\infty}^{\infty}|\kappa_{i_1\cdots i_\ell}^{j_1\cdots j_\ell}(s_2,\ldots,s_\ell;d_1,\ldots,d_\ell)|\\
&= O(n^{-\ell/2+1}),
\end{aligned} \tag{A.1}$$

where $\overline{e_{ij.d}} := \sum_{t=1}^{n_{ij}} e_{ijtd}/n_{ij}$ for any $(i,j,d) \in \{1,\ldots,a\}\times\{1,\ldots,b\}\times\{1,\ldots,p\}$. From these observations, we conclude, under H_α, that

$$\sqrt{n}\left(\overline{\boldsymbol{y}_{1..}}^\top - \overline{\boldsymbol{y}_{...}}^\top \quad \ldots \quad \overline{\boldsymbol{y}_{a..}}^\top - \overline{\boldsymbol{y}_{...}}^\top\right)^\top \Rightarrow N(\boldsymbol{0},\boldsymbol{V}_\alpha) \quad \text{as } \min_{\substack{i=1,\ldots,a\\j=1,\ldots,b}} n_{ij} \to \infty.$$

Koliha (2001, Corollary 1.8) and (A3) yield that $\hat{\boldsymbol{V}}_{n,\alpha}^-$ converges in probability to $\boldsymbol{V}_\alpha^-$ as $\min_{\substack{i=1,\ldots,a\\j=1,\ldots,b}} n_{ij} \to \infty$. The conclusion of the theorem then follows from Lemma A.1. ■

A.2 Proof of Theorem 22

Theorem 2.1 gives that $\left(\overline{\boldsymbol{e}_{1..}}^\top - \overline{\boldsymbol{e}_{...}}^\top \quad \ldots \quad \overline{\boldsymbol{e}_{a..}}^\top - \overline{\boldsymbol{e}_{...}}^\top\right)^\top = O_p(1/\sqrt{n})$. It follows, under K_α, that, for any $i_1, i_2 \in \{1,\ldots,a\}$,

$$\begin{aligned}
& \mathbb{P}(T_{n,\alpha} \geq \chi^2_{\hat{r}_{n,\alpha}}[1-\tau])\\
= \; & \mathbb{P}(T_{n,\alpha}/n \geq \chi^2_{r_\alpha}[1-\tau]/n) + o_p(1)\\
\to \; & \mathbb{P}\Big(\left(\boldsymbol{\alpha}_1{}^\top - \overline{\boldsymbol{\alpha}}_\cdot{}^\top \quad \ldots \quad \boldsymbol{\alpha}_a{}^\top - \overline{\boldsymbol{\alpha}}_\cdot{}^\top\right)\boldsymbol{V}_\alpha^-\left(\boldsymbol{\alpha}_1{}^\top - \overline{\boldsymbol{\alpha}}_\cdot{}^\top \quad \ldots \quad \boldsymbol{\alpha}_a{}^\top - \overline{\boldsymbol{\alpha}}_\cdot{}^\top\right)^\top \geq 0\Big) \quad \text{as } \min_{\substack{i=1,\ldots,a\\j=1,\ldots,b}} n_{ij} \to \infty.
\end{aligned}$$

The most right hand side is equal to one since the Moore–Penrose inverse of any nonnegative definite matrix is nonnegative definite (Wu, 1980, Theorem 1). Thus, we obtain the desired results. ■

A.3 Proof of Theorem 23

The proof will be completed by the continuous mapping theorem once we show, under $K_\alpha^{(n)}$, that

$$\sqrt{n}\left(\overline{\boldsymbol{y}_{1..}}^\top - \overline{\boldsymbol{y}_{...}}^\top \quad \ldots \quad \overline{\boldsymbol{y}_{a..}}^\top - \overline{\boldsymbol{y}_{...}}^\top\right)^\top \Rightarrow N(\boldsymbol{0},{}^{\alpha}\tilde{\boldsymbol{H}}+\boldsymbol{V}_\alpha) \quad \text{as } \min_{\substack{i=1,\ldots,a\\j=1,\ldots,b}} n_{ij} \to \infty.$$

For any $i \in \{1, \ldots, a\}$, it holds that $\sqrt{n}\mathbb{E}(\overline{\boldsymbol{y}_{i\cdot\cdot}} - \overline{\boldsymbol{y}_{\cdots}}) = \boldsymbol{0}$. It can be shown that, for any $i_1, i_2 \in \{1, \ldots, a\}$,

$$
\begin{aligned}
n\mathrm{Cov}(\overline{\boldsymbol{y}_{i_1\cdot\cdot}} - \overline{\boldsymbol{y}_{\cdots}}, \overline{\boldsymbol{y}_{i_2\cdot\cdot}} - \overline{\boldsymbol{y}_{\cdots}}) &= n\mathrm{Cov}(\boldsymbol{\alpha}_{i_1} - \overline{\boldsymbol{\alpha}_{\cdot}}, \boldsymbol{\alpha}_{i_2} - \overline{\boldsymbol{\alpha}_{\cdot}}) + n\mathrm{Cov}(\overline{\boldsymbol{e}_{i_1\cdot\cdot}} - \overline{\boldsymbol{e}_{\cdots}}, \overline{\boldsymbol{e}_{i_2\cdot\cdot}} - \overline{\boldsymbol{e}_{\cdots}}) \\
&= {}^{\alpha}\tilde{\boldsymbol{H}}_{i_1 i_2} + {}^{n,\alpha}\boldsymbol{V}_{i_1 i_2},
\end{aligned}
$$

where

$$
{}^{\alpha}\tilde{\boldsymbol{H}}_{i_1 i_2} := {}^{\alpha}\boldsymbol{H}_{i_1 i_2} - \frac{1}{a}\sum_{s=1}^{a}({}^{\alpha}\boldsymbol{H}_{i_1 s} + {}^{\alpha}\boldsymbol{H}_{s i_2}) + \frac{1}{a^2}\sum_{s_1, s_2 = 1}^{a} {}^{\alpha}\boldsymbol{H}_{s_1 s_2}.
$$

Since $\{\boldsymbol{\alpha}_i\}$ is normally distributed, third and higher-order cumulants are zero. In conjunction with (A.1), we conclude the theorem. ■

A.4 Proof of Theorem 31–33

The proofs of Theorem 31–33 can be shown along the lines with the proofs of Theorem 21–23. So the proofs are omitted. ■

B Additional simulation results.

In this section, we provide additional simulation results for the tests. The settings of the simulation are described in the main manuscript.

Figures 1 and 2 illustrate the empirical size and power for the test for existence of random effects defined in (2.2). Similarly, Figures 3 and 4 show the empirical size and power for the test for existence of random effects defined in (3.2). Note that the scale of vertical axes of Figures for $\sigma_\alpha = 0$ and $\sigma_\gamma = 0$ are differ from other Figures. For the results for some parameters in the MA model, $n = 1000$ provides better size control than $n = 2000$ under the null, e.g., $(c_1, c_2) = (-0.1, 0.4), (0, -0.4), (0.1, -0.1)$ with a normal distribution in Figure 1. A similar tendency, though less pronounced, can be also seen in the results for some parameters in the AR model. Overall, our tests have good size control under the null and reasonable power under the alternative.

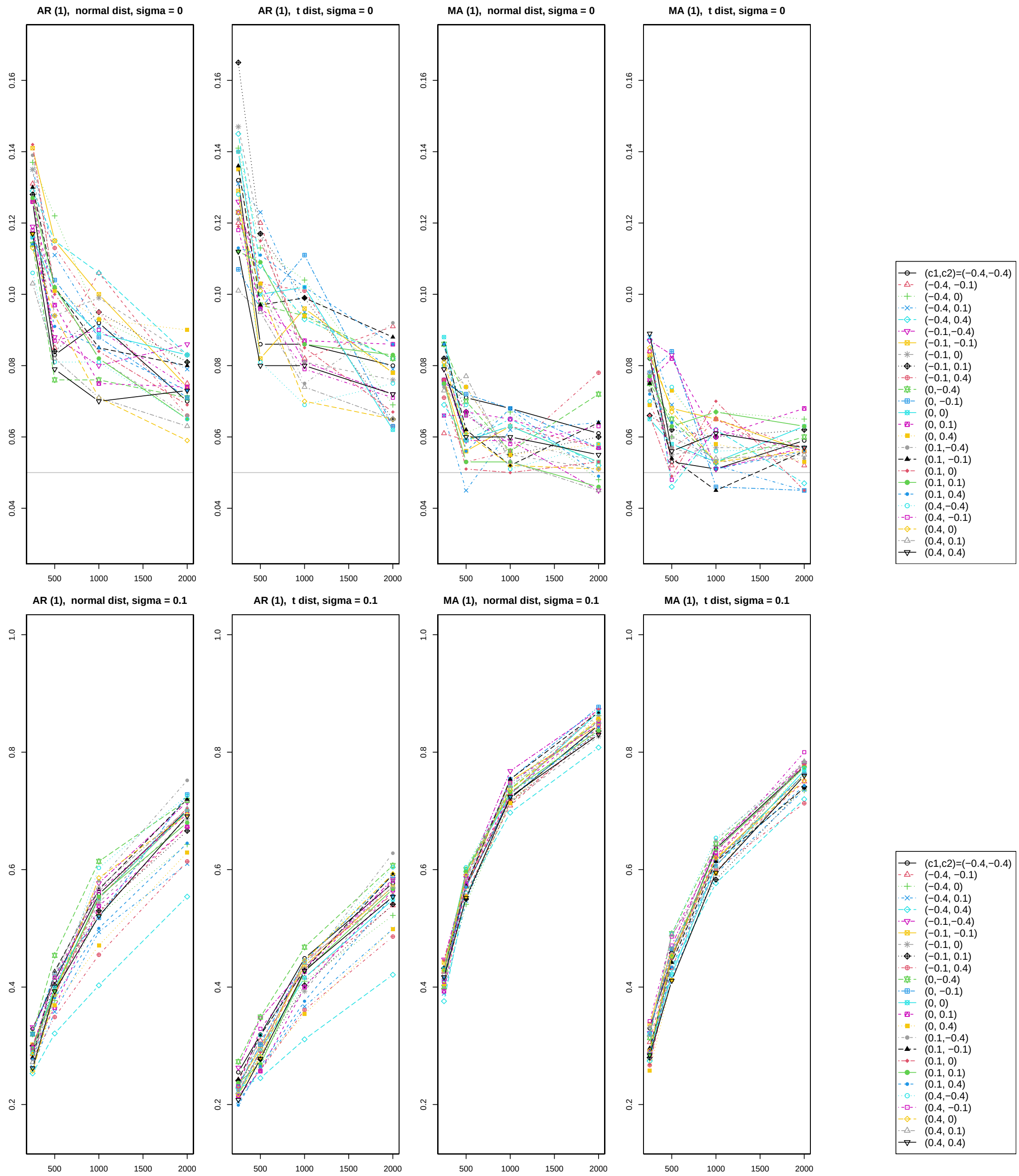

Figure 1: Empirical size and power for the hypothesis defined in (2.2) for $\sigma_\alpha = 0, 0.1$. The vertical and horizontal axes correspond to the rejection probabilities over 1000 iterations and time series lengths, respectively. The upper and lower figures correspond to the null ($\sigma_\alpha = 0$) and the alternative ($\sigma_\alpha = 0.1$), respectively. The first and second columns correspond to results for AR(1) models whose disturbances follow the normal distribution and the t-distribution with 5 degrees of freedom, respectively. The third and four columns correspond to results for MA(1) models whose disturbances follow the normal distribution and the t-distribution with 5 degrees of freedom, respectively.

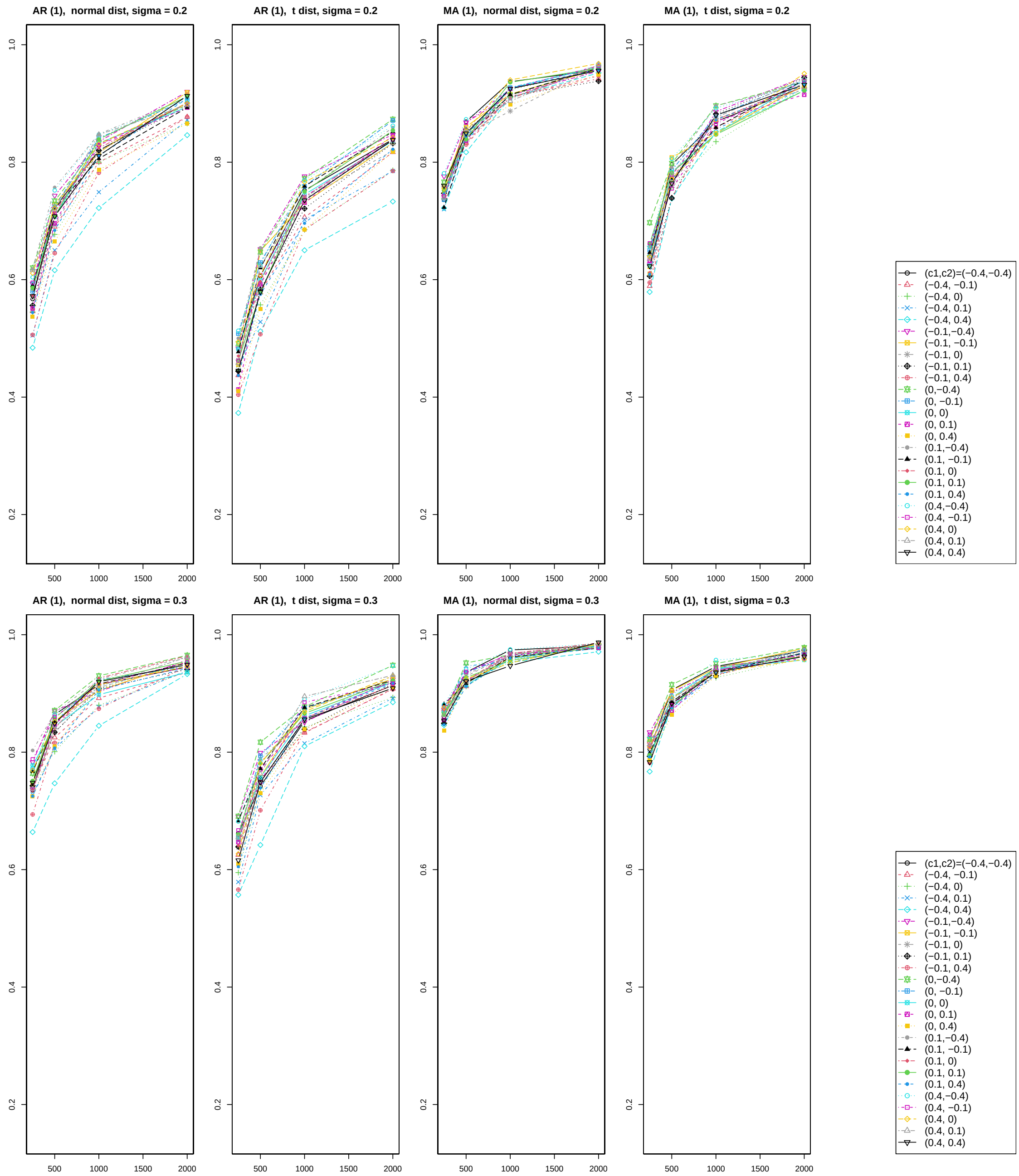

Figure 2: Empirical power for the hypothesis defined in (2.2) for $\sigma_\alpha = 0.2, 0.3$. The vertical and horizontal axes correspond to the rejection probabilities over 1000 iterations and time series lengths, respectively. The upper and lower figures correspond to the alternative ($\sigma_\alpha = 0.2, 0.3$). The first and second columns correspond to results for AR(1) models whose disturbances follow the normal distribution and the t-distribution with 5 degrees of freedom, respectively. The third and four columns correspond to results for MA(1) models whose disturbances follow the normal distribution and the t-distribution with 5 degrees of freedom, respectively.

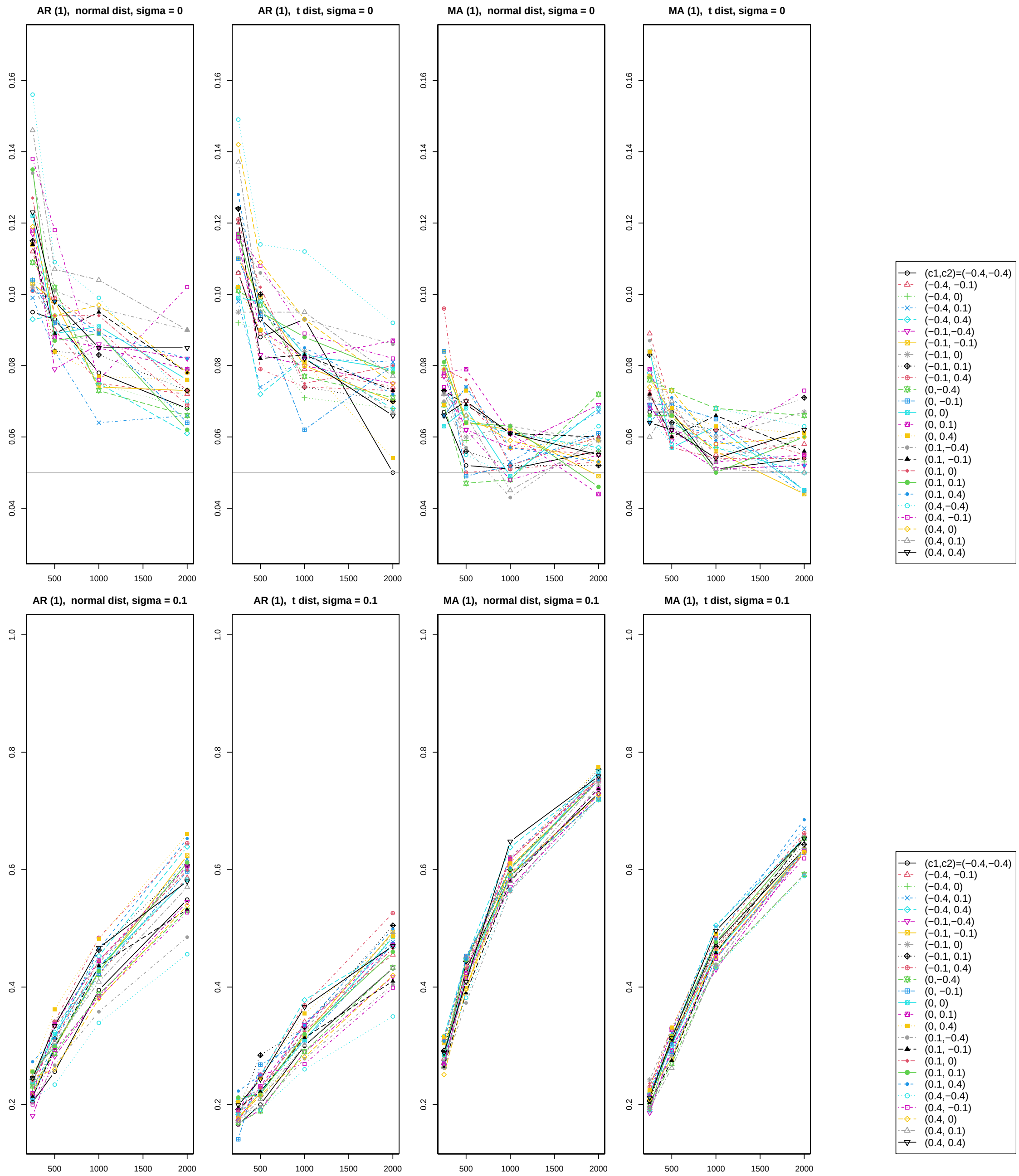

Figure 3: Empirical size and power for the hypothesis defined in (3.2) for $\sigma_\gamma = 0, 0.1$. The vertical and horizontal axes correspond to the rejection probabilities over 1000 iterations and time series lengths, respectively. The upper and lower figures correspond to the null ($\sigma_\gamma = 0$) and the alternative ($\sigma_\alpha = 0.1$), respectively. The first and second columns correspond to results for AR(1) models whose disturbances follow the normal distribution and the t-distribution with 5 degrees of freedom, respectively. The third and four columns correspond to results for MA(1) models whose disturbances follow the normal distribution and the t-distribution with 5 degrees of freedom, respectively.

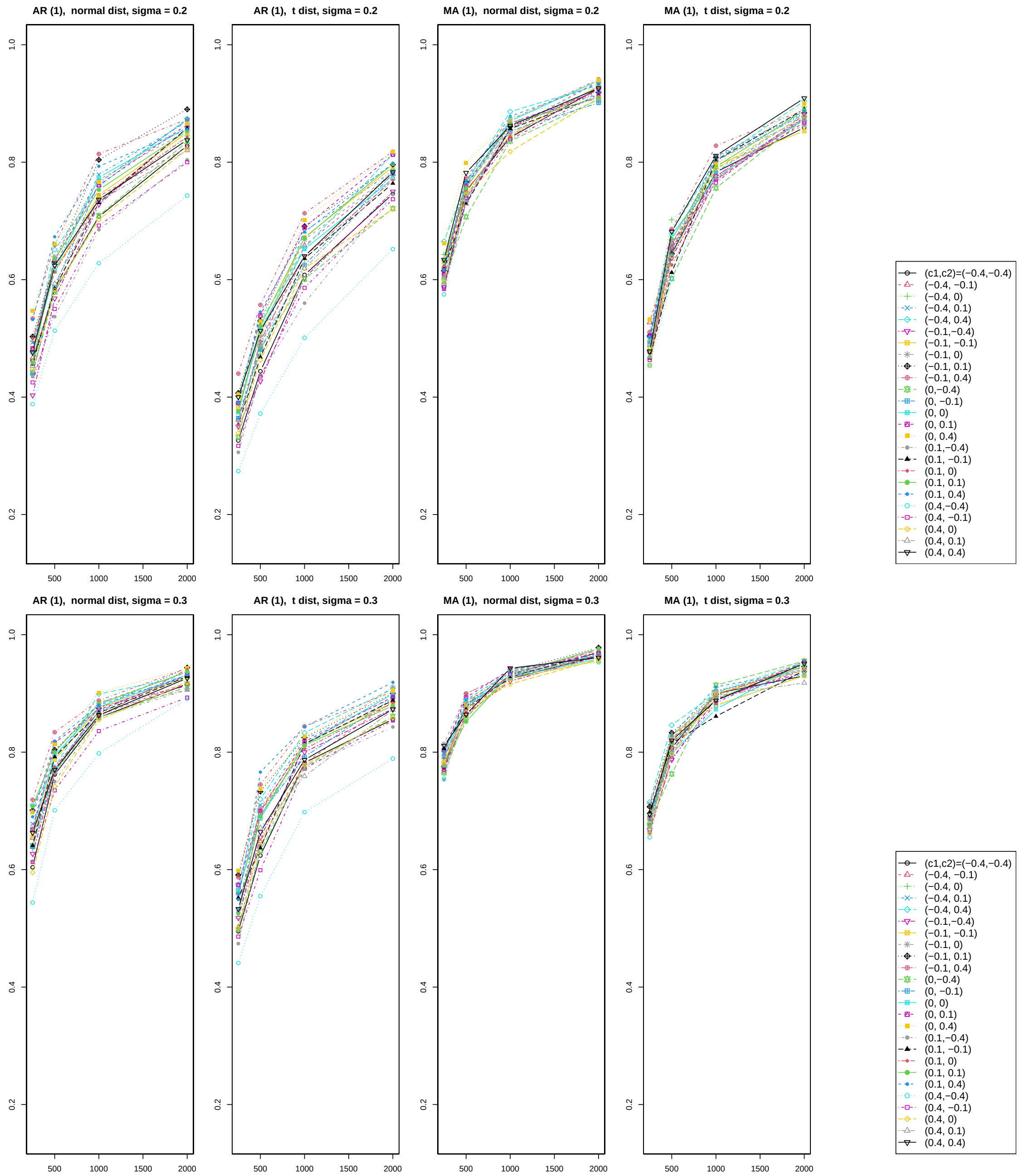

Figure 4: Empirical power for the hypothesis defined in (3.2) for $\sigma_\gamma = 0.2, 0.3$. The vertical and horizontal axes correspond to the rejection probabilities over 1000 iterations and time series lengths, respectively. The upper and lower figures correspond to the alternative ($\sigma_\gamma = 0.2, 0.3$). The first and second columns correspond to results for AR(1) models whose disturbances follow the normal distribution and the t-distribution with 5 degrees of freedom, respectively. The third and four columns correspond to results for MA(1) models whose disturbances follow the normal distribution and the t-distribution with 5 degrees of freedom, respectively.

References

Koliha, J. (2001). Continuity and differentiability of the Moore-Penrose inverse in C*-algebras. *Mathematica Scandinavica* **88** 154–160.

Rao, C. R. and Mitra, S. K. (1971). *Generalized inverse of matrices and its applications*. New York: Wiley.

Wu, C.-F. (1980). On some ordering properties of the generalized inverses of nonnegative definite matrices. *Linear Algebra and its Applications* **32** 49–60.